



HAL
open science

Tsunami wave energy

Denys Dutykh, Frédéric Dias

► **To cite this version:**

| Denys Dutykh, Frédéric Dias. Tsunami wave energy. 2008. hal-00311752v1

HAL Id: hal-00311752

<https://hal.science/hal-00311752v1>

Preprint submitted on 20 Aug 2008 (v1), last revised 22 Oct 2008 (v2)

HAL is a multi-disciplinary open access archive for the deposit and dissemination of scientific research documents, whether they are published or not. The documents may come from teaching and research institutions in France or abroad, or from public or private research centers.

L'archive ouverte pluridisciplinaire **HAL**, est destinée au dépôt et à la diffusion de documents scientifiques de niveau recherche, publiés ou non, émanant des établissements d'enseignement et de recherche français ou étrangers, des laboratoires publics ou privés.

Tsunami wave energy

BY DENYS DUTYKH, FRÉDÉRIC DIAS

*CMLA, ENS Cachan, CNRS, PRES UniverSud, 61, avenue du Président Wilson,
94230 Cachan cedex, France*

In the vast literature on tsunami research, few articles have been devoted to energy issues. A theoretical investigation on the energy of waves generated by bottom motion is performed here. We start with the full incompressible Euler equations in the presence of a free surface and derive both dispersive and non-dispersive shallow-water equations with an energy equation. It is shown that dispersive effects only appear at higher order in the energy budget. Then we solve the Cauchy–Poisson problem of tsunami generation for the linearized water wave equations. Exchanges between potential and kinetic energies are clearly revealed.

Keywords: water waves, shallow-water equations, tsunami energy

1. Introduction

Oceanic waves can be devastating as shown by recent events. Whilst some areas are more vulnerable than others, the recent history shows that catastrophic waves can hit even where they are not expected. The tsunami waves generated by the huge undersea earthquake in Indonesia on 26 December 2004 caused devastation across most of the coasts of the Bay of Bengal. The tsunami waves generated by the massive submarine landslide in Papua-New Guinea on 17 July 1998 as well as the 17 July 2006 Java tsunami and the 2 April 2007 Solomon Islands tsunami also caused devastation, but on a smaller scale. Unfortunately, such cataclysmic tsunamis are likely to be generated again by earthquakes, massive landslides or volcano eruptions [Synolakis and Bernard, 2006].

Information on tsunami energy can be obtained by applying the normal mode representation of tsunami waves, as introduced by Ward [1980]. For example, Okal [2003] considers the total energy released into tsunami waves. He obtains expressions for the energy of tsunamis (see his expressions (31) for a tsunami generated by an earthquake and (36) for a tsunami generated by a landslide). In the case of a landslide, he computes the ratio between tsunami energy and total change in energy due to the slide. In the present paper, we will use the incompressible fluid dynamics equations. Tsunamis have traditionally been considered as non-dispersive long waves. However various types of data (bottom pressure records [Ritsema et al., 1995]; satellite data [Kulikov et al., 2005]; hydrophone records [Okal et al., 2007]) indicate that tsunamis are made up of a very long dispersive wave train, especially when they have enough time to propagate. These waves travel across the ocean surface in all directions away from the generation region. Recent numerical computations using dispersive wave models such as the Boussinesq equations show as much as 20% reduction of tsunami amplitude in certain locations due to dispersion

[Dao and Tkalich, 2007]. But one has to be careful with the interpretation of satellite data: as indicated by K anoglu and Synolakis [2006], the mid-ocean steepness of the 2004 Sumatra tsunami measured from satellite altimeter data was less than 10^{-5} . Nonlinear dispersive theory is necessary only when examining steep gravity waves, which is not the case in deep water.

The wavelength of tsunamis and, consequently, their period depend essentially on the source mechanism. If the tsunami is generated by a large and shallow earthquake, its initial wavelength and period will be greater. On the other hand, if the tsunami is caused by a landslide (which happens less commonly but can be devastating as well), both its initial wavelength and period will be shorter. From these empirical considerations one can conclude that dispersive effects are a priori more important for submarine landslide and slump scenarios than for tsunamigenic earthquakes.

Once a tsunami has been generated, its energy is distributed throughout the water column. Clearly, the more water is displaced, the more energetic is the tsunami (compare for example the December 2004 and March 2005 Sumatra tsunamis). Due to the large scale of this natural phenomenon and limited power of computers, tsunami wave modellers have to adopt simplified models which reduce a fully three-dimensional (3D) problem to a two-dimensional (2D) one. This approach is natural, since in the case of very long waves the water column moves as a whole. Consequently the flow is almost 2D. Among these models one can mention the nonlinear shallow water equations (SWE), Boussinesq type models, the Green-Naghdi and Serre equations. There is a wide variety of models, depending on whether or not the effects of run-up/run-down, bottom friction, turbulence, Coriolis effects, tidal effects, etc, are included.

Today scientists can easily predict when a tsunami will arrive at various places by knowing source characteristics and bathymetry data along the paths to those places. Unfortunately one does not know as much about the energy propagation of such waves. Obviously tsunami amplitude is enhanced over the major oceanic ridges. Titov et al. [2005] clearly describe the waveguide type effect from mid-ocean ridges that has funnelled the 2004 megatsunami away from the tip of Africa. As emphasized by Kowalik et al. [2007], travel-time computation based on the first arrival time may lead to errors in the prediction of tsunami arrival time as higher energy waves propagate slower along ridges. At the beginning, the energy is essentially potential, although it depends on the generation mechanism. Then it redistributes itself into half kinetic and half potential energies. Finally, it converts its potential component into kinetic energy. How do these conversions take place? The purpose of this study is to shed some light on this topic and to see if the importance of dispersion in tsunamis can be studied by looking at the energy rather than at wave profiles.

Previous researchers have considered this topic. Kajiura [1970] studied the energy exchange associated with the bottom deformation between the solid bottom and the overlying water. There were recent attempts to obtain equations for tsunami energy propagation. We can mention here the work of Tinti and Bortolucci [2000] devoted to idealized theoretical cases and the work of Kowalik et al. [2007] using the energy flux point of view to study the changes in the 2004 tsunami signal as it travelled from Indonesia to the Pacific Ocean. We believe that these models can be improved, given the present state of the art in wave modelling.

A point of interest is that some of the equations used for wave modelling have an infinite number of conserved quantities. There has been some confusion in the literature on which quantities can be called energy. Indeed there is here an interesting question. In incompressible fluid mechanics, the internal energy equation is decoupled from the equation of continuity and from the fundamental law of dynamics. It is used only when one is interested in computing the temperature field once the velocity distribution is known. In addition to the internal energy equation, one can write a total energy (internal energy + kinetic energy) equation, or a total enthalpy equation. The confusing part is that for perfect fluids one usually defines the total energy differently: it is the sum of internal energy, kinetic energy, and potential energies associated to body forces such as gravitational forces and to the pressure field. If in addition the fluid is incompressible, then the internal energy remains constant. In the classical textbooks on water waves [Johnson, 1997, Stoker, 1958], one usually introduces the energy E as the sum of kinetic and potential energies and then looks for a partial differential equation giving the time derivative dE/dt (incidentally the meaning of d/dt is not always clearly defined). In any case, when one uses a depth-integrated model such as the nonlinear SWE, one can compute the energy a posteriori (the potential energy is based on the free-surface elevation and the kinetic energy on the horizontal velocity). But one can also apply the nonlinear shallow water assumptions to the full energy equation to begin with. Then one obtains a nonlinear shallow water approximation of the energy equation. Are these two approaches equivalent? We show that the answer is no.

First we present the energy equation in three different forms: full water wave equations, dispersive SWE and non-dispersive SWE. Surprisingly, the energy equation is the same for dispersive and non-dispersive SWE at leading order. Then we present some numerical computations over a flat bottom. It allows us to concentrate on the generation process and the energy transfer through the moving seabed. We refer to Duytkh et al. [2008] for simulations of some real world events including energy pumping and its transformation over uneven bathymetry, using the SWE with energy. Finally the Cauchy–Poisson problem of tsunami generation for the linearized water wave equations is solved. Exchanges between potential and kinetic energies are clearly revealed.

2. Derivation of the energy equation

Consider the 3D fluid domain shown in Figure 1. It is bounded above by the free surface $z^* = \eta^*(x^*, y^*, t^*)$ and below by the rigid boundary with prescribed motion $z^* = -h^*(x^*, y^*, t^*)$. A Cartesian coordinate system with the z^* -axis pointing vertically upwards and the xOy -plane coinciding with the still-water level is chosen.

The fluid is assumed to be inviscid. Its motion is governed by the 3D Euler equations, written here in their incompressible form (see Gisler [2008] for the compressible counterpart, after replacing ρ by p in the pressure term of his Eq. 3):

$$\nabla \cdot \mathbf{u}^* = 0, \quad (2.1)$$

$$\frac{\partial \mathbf{u}^*}{\partial t^*} + \nabla \cdot \left(\mathbf{u}^* \otimes \mathbf{u}^* + \frac{p^*}{\rho^*} \text{Id} \right) = \mathbf{g}, \quad (2.2)$$

$$\frac{\partial e^*}{\partial t^*} + \nabla \cdot \left[\left(e^* + \frac{p^*}{\rho^*} \right) \mathbf{u}^* \right] = 0, \quad (2.3)$$

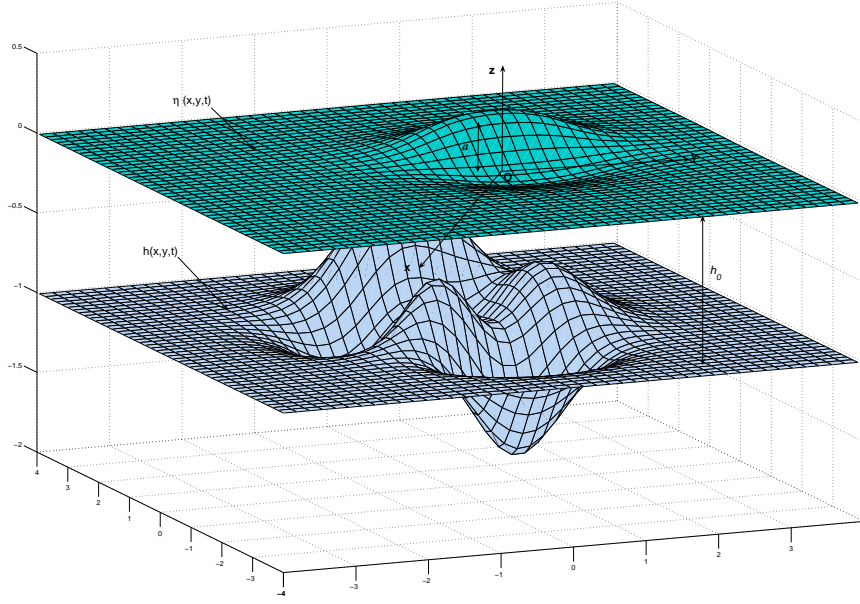


Figure 1. Sketch of the fluid domain for wave generation by a moving bottom

where ρ^* is the fluid density, $\mathbf{u}^* = (u^*, v^*, w^*)$ the velocity vector, e^* the sum of kinetic energy density $e_K^* = \frac{1}{2} |\mathbf{u}^*|^2$ and potential energy density $e_P^* = gz^*$, p^* the pressure and \mathbf{g} the acceleration due to gravity. In the present study $\mathbf{g} = (0, 0, -g)$. For incompressible flows, the energy equation (2.3) is redundant. Indeed it can be obtained from Eq. (2.2). However we keep it since it is not equivalent to derive shallow water equations with or without the energy equation.

Equations (2.1)–(2.3) have to be completed by the kinematic and dynamic boundary conditions. Since surface tension effects are not important for long waves, the dynamic boundary condition on the free surface reads

$$p^* = p_s^*, \quad \text{at } z^* = \eta^*. \quad (2.4)$$

Later we will replace the surface pressure p_s^* by 0 but we keep it arbitrary for now.

The kinematic boundary conditions on the free surface and at the seabed are, respectively,

$$w^* = \frac{\partial \eta^*}{\partial t^*} + u^* \frac{\partial \eta^*}{\partial x^*} + v^* \frac{\partial \eta^*}{\partial y^*}, \quad z^* = \eta^*, \quad (2.5)$$

$$w^* = -\frac{\partial h^*}{\partial t^*} - u^* \frac{\partial h^*}{\partial x^*} - v^* \frac{\partial h^*}{\partial y^*}, \quad z^* = -h^*. \quad (2.6)$$

Below we denote the horizontal gradient by ∇_{\perp} and the horizontal velocity by \mathbf{u}_{\perp}^* . After a few manipulations and integration across the water column from bottom to top, one can write the following global energy equation:

$$\frac{\partial E^*}{\partial t^*} + \nabla_{\perp} \cdot \Phi^* + P^* = 0, \quad (2.7)$$

where E^* is the sum of kinetic and potential energies in the flow, per unit horizontal area, Φ^* the horizontal energy flux vector, and P^* the net energy input due to the

pressure forces doing work on the upper and lower boundaries of the fluid. They are given by the following expressions:

$$E^* = \int_{-h^*}^{\eta^*} \left(\frac{1}{2} \rho^* |\mathbf{u}^*|^2 + \rho^* g z^* \right) dz^*, \quad (2.8)$$

$$\Phi^* = \int_{-h^*}^{\eta^*} \mathbf{u}_\perp^* \left(\frac{1}{2} \rho^* |\mathbf{u}^*|^2 + p^* + \rho^* g z^* \right) dz^*, \quad (2.9)$$

$$P^* = p_s^* \eta_{t^*}^* + p_b^* h_{t^*}^*, \quad (2.10)$$

where p_s^* is the pressure exerted on the free surface and p_b^* the bottom pressure. In the case of a stationary bottom boundary and of a free surface on which the pressure vanishes, then as expected the net energy input P^* is identically zero. Energy can be brought to the system by a moving bottom or by a pressure disturbance on the free surface. From now on, we take $p_s^* = 0$.

(a) *Dimensionless equations*

The problem of tsunami propagation possesses two characteristic length scales: the average water depth h_0 for the vertical dimension and a typical wavelength l for the horizontal dimensions. It is classical to introduce the following dimensionless variables. The scaling for the independent variables is

$$x = \frac{x^*}{l}, \quad y = \frac{y^*}{l}, \quad z = \frac{z^*}{h_0}, \quad t = \frac{\sqrt{gh_0}}{l} t^*.$$

In order to introduce the dimensionless dependent variables we need one more parameter, the typical wave amplitude a :

$$u = \frac{h_0}{a\sqrt{gh_0}} u^*, \quad v = \frac{h_0}{a\sqrt{gh_0}} v^*, \quad w = \frac{h_0}{l} \frac{h_0}{a\sqrt{gh_0}} w^*, \quad \eta = \frac{\eta^*}{a}, \quad h = \frac{h^*}{h_0},$$

$$\pi = \frac{p^* + \rho^* g z^*}{\rho^* g a}, \quad p = \frac{p^*}{\rho^* g h_0}, \quad e = \frac{e^*}{g h_0}.$$

The hydrostatic pressure $-\rho^* g z^*$ has been incorporated into π .

The following dimensionless parameters, which are assumed to be small, are introduced:

$$\varepsilon := a/h_0, \quad \mu := h_0/l.$$

The parameter ε represents the relative importance of nonlinear terms and μ measures dispersive effects. Note that

$$e = \frac{1}{2} \varepsilon^2 (u^2 + v^2) + \frac{1}{2} \frac{\varepsilon^2}{\mu^2} w^2 + z.$$

The Euler equations of motion (2.1)–(2.3) become in dimensionless form

$$\mu^2 (u_x + v_y) + w_z = 0 \quad (2.11)$$

$$\mu^2 u_t + \varepsilon \mu^2 (u^2)_x + \varepsilon \mu^2 (uv)_y + \varepsilon (uw)_z + \mu^2 \pi_x = 0, \quad (2.12)$$

$$\mu^2 v_t + \varepsilon \mu^2 (uv)_x + \varepsilon \mu^2 (v^2)_y + \varepsilon (vw)_z + \mu^2 \pi_y = 0, \quad (2.13)$$

$$\mu^2 w_t + \varepsilon \mu^2 (uw)_x + \varepsilon \mu^2 (vw)_y + \varepsilon (w^2)_z + \mu^2 \pi_z = 0, \quad (2.14)$$

$$\mu^2 e_t + \varepsilon \mu^2 ((e+p)u)_x + \varepsilon \mu^2 ((e+p)v)_y + \varepsilon ((e+p)w)_z = 0. \quad (2.15)$$

In dimensionless form the boundary conditions (2.4), (2.5) and (2.6) become

$$\pi = \eta, \quad z = \varepsilon \eta, \quad (2.16)$$

$$w = \mu^2 \eta_t + \varepsilon \mu^2 u \eta_x + \varepsilon \mu^2 v \eta_y, \quad z = \varepsilon \eta, \quad (2.17)$$

$$\varepsilon w = -\mu^2 h_t - \varepsilon \mu^2 u h_x - \varepsilon \mu^2 v h_y, \quad z = -h. \quad (2.18)$$

In the case of a static bottom $h = h(x, y)$, the vertical velocity at the bottom $w = O(\mu^2)$. With a moving bathymetry the behaviour is different:

$$w = -\frac{\mu^2}{\varepsilon} h_t + O(\mu^2).$$

(b) *Integration over the depth*

Next we reduce the above 3D problem (2.11)–(2.18) into a 2D one by integrating all the equations over the water column. We begin with the continuity equation (2.11) which we integrate with respect to z from $-h$ to $\varepsilon \eta$. Taking into account the boundary conditions (2.17) and (2.18), one obtains

$$\eta_t + \frac{\partial}{\partial x} \int_{-h}^{\varepsilon \eta} u \, dz + \frac{\partial}{\partial y} \int_{-h}^{\varepsilon \eta} v \, dz = -\frac{1}{\varepsilon} h_t. \quad (2.19)$$

A source term appears in equation (2.19) due to the moving bathymetry. For tsunami generation, the function h^* can be represented as follows:

$$h^*(x^*, y^*, t^*) = h_0^*(x^*, y^*) - \zeta^*(x^*, y^*, t^*),$$

where $h_0^*(x^*, y^*)$ is the static sea bed profile and $\zeta^*(x^*, y^*, t^*)$ the bottom displacement due for example to coseismic displacements or landslides. In nondimensional form this representation takes the form:

$$h(x, y, t) = h_0(x, y) - \varepsilon \zeta(x, y, t),$$

since the bottom variation must be of the same order of magnitude as the typical wave amplitude a : $\zeta^*(x^*, y^*, t^*) = a \zeta(x, y, t)$. Differentiating with respect to time yields

$$\frac{1}{\varepsilon} \frac{\partial h}{\partial t} = -\frac{\partial \zeta}{\partial t} = O(1).$$

Below we will replace $\frac{1}{\varepsilon} h_t$ by $-\zeta_t$.

Integrating the vertical momentum conservation equation (2.14) yields

$$\pi|_{z=-h} = \eta + \frac{\partial}{\partial t} \int_{-h}^{\varepsilon \eta} w \, dz + \varepsilon \frac{\partial}{\partial x} \int_{-h}^{\varepsilon \eta} uw \, dz + \varepsilon \frac{\partial}{\partial y} \int_{-h}^{\varepsilon \eta} vw \, dz. \quad (2.20)$$

A more general expression for the pressure can be obtained if we integrate equation (2.14) from z to $\varepsilon\eta$ and use boundary conditions (2.16) and (2.17):

$$\pi = \eta + \frac{\partial}{\partial t} \int_z^{\varepsilon\eta} w \, dz + \varepsilon \frac{\partial}{\partial x} \int_z^{\varepsilon\eta} uw \, dz + \varepsilon \frac{\partial}{\partial y} \int_z^{\varepsilon\eta} vw \, dz - \frac{\varepsilon}{\mu^2} w^2. \quad (2.21)$$

The vertical velocity w is obtained by integrating the continuity equation (2.11) from $-h$ to z and applying the seabed kinematic condition (2.18):

$$w = \mu^2 \zeta_t - \mu^2 \left(\frac{\partial}{\partial x} \int_{-h}^z u \, dz + \frac{\partial}{\partial y} \int_{-h}^z v \, dz \right). \quad (2.22)$$

Finally, the integration of the equation of energy conservation (2.15) yields

$$\frac{\partial}{\partial t} \int_{-h}^{\varepsilon\eta} e \, dz + \varepsilon \frac{\partial}{\partial x} \int_{-h}^{\varepsilon\eta} (e + p)u \, dz + \varepsilon \frac{\partial}{\partial y} \int_{-h}^{\varepsilon\eta} (e + p)v \, dz - \varepsilon p|_{z=-h} \zeta_t = 0, \quad (2.23)$$

which is nothing else than the dimensionless counterpart of equation (2.7).

All the equations derived above are exact and no assumption has been made about the orders of magnitude of ε and μ .

(c) *The nonlinear shallow-water equations with energy equation*

In Appendix A, we briefly summarize the derivation of various systems of shallow-water wave equations. The non-dispersive SWE are obtained by taking the limit $\mu \rightarrow 0$. Here we provide the dispersive and non-dispersive SWE in their conservative forms [Eskilsson and Sherwin, 2005] with dimensions, based on the depth-averaged horizontal velocity $\bar{\mathbf{u}}^*$. The total water depth $h^* + \eta^*$ is denoted by $H^*(x^*, y^*, t^*)$. The definition of E^* is given by Eq. (2.8).

(i) *SWE with dispersion and energy equation*

$$\frac{\partial H^*}{\partial t^*} + \nabla \cdot (H^* \bar{\mathbf{u}}^*) = 0, \quad (2.24)$$

$$\begin{aligned} & \frac{\partial (H^* \bar{\mathbf{u}}^*)}{\partial t^*} + \nabla \cdot \left(H^* \bar{\mathbf{u}}^* \otimes \bar{\mathbf{u}}^* + \frac{1}{2} g H^{*2} \right) + \\ & \left(\frac{h^{*3}}{6} \nabla \cdot \left(\nabla \cdot \left(\frac{H^* \bar{\mathbf{u}}^*}{h^*} \right) \right) - \frac{h^{*2}}{2} \nabla \cdot (\nabla \cdot (H^* \bar{\mathbf{u}}^*)) \right)_{t^*} = g H^* \nabla h^*, \end{aligned} \quad (2.25)$$

$$\frac{\partial E^*}{\partial t^*} + \nabla \cdot \left(\bar{\mathbf{u}}^* \left(E^* + \frac{1}{2} \rho^* g H^{*2} \right) \right) = \rho^* g H^* \frac{\partial \zeta^*}{\partial t^*}. \quad (2.26)$$

(ii) *SWE without dispersion and with energy equation*

$$\frac{\partial H^*}{\partial t^*} + \nabla \cdot (H^* \bar{\mathbf{u}}^*) = 0, \quad (2.27)$$

$$\frac{\partial (H^* \bar{\mathbf{u}}^*)}{\partial t^*} + \nabla \cdot \left(H^* \bar{\mathbf{u}}^* \otimes \bar{\mathbf{u}}^* + \frac{1}{2} g H^{*2} \right) = g H^* \nabla h^*, \quad (2.28)$$

$$\frac{\partial E^*}{\partial t^*} + \nabla \cdot \left(\bar{\mathbf{u}}^* \left(E^* + \frac{1}{2} \rho^* g H^{*2} \right) \right) = \rho^* g H^* \frac{\partial \zeta^*}{\partial t^*}. \quad (2.29)$$

Between (i) and (ii), only the equation for the evolution of the horizontal velocity (2.28) differs. In particular, it is interesting to note that the energy equations are the same in the dispersive and non-dispersive cases. Differences appear only at higher order (terms of order $O(\varepsilon\mu^2)$). An additional remark can be made about the hyperbolic structure of the system (2.27)–(2.29). We restrict our observations to one space dimension. Let us assume that a shock wave propagates from left to right at velocity $s > 0$. The states before and after the discontinuity are denoted by $(H_{l,r}^*, \bar{u}_{l,r}^*, E_{l,r}^*)$ correspondingly. From entropy considerations one can conclude that for an admissible state $H_l^* > H_r^*$. For a general system of conservation laws $v_t + \partial_x f(v) = 0$, the Rankine-Hugoniot relations have the simple form $f(v_r) - f(v_l) = s(v_r - v_l)$.

Some simple algebraic calculations yield the following relations:

$$s = \frac{H_l^* \bar{u}_l^* - H_r^* \bar{u}_r^*}{H_l^* - H_r^*}, \quad \bar{u}_r^* = \bar{u}_l^* \pm \sqrt{\frac{1}{2} g (H_l^{*2} - H_r^{*2}) \left(\frac{1}{H_r^*} - \frac{1}{H_l^*} \right)},$$

$$\frac{E_r^*}{H_r^*} = \frac{E_l^*}{H_l^*} - \frac{1}{2} \rho^* g \left(\frac{1}{H_r^*} - \frac{1}{H_l^*} \right) \frac{H_r^{*2} \bar{u}_r^* - H_l^{*2} \bar{u}_l^*}{\bar{u}_r^* - \bar{u}_l^*}. \quad (2.30)$$

These formulas relate left and right states connected in the (H^*, \bar{u}^*, E^*) space by a shock wave. The first two relations are well known. What is new to our knowledge is the formula (2.30) which gives an insight into the energy states in a shock wave. In practice, they can be used for the theoretical analysis of bores and as a validation test for nonlinear SWE codes (with energy equation).

3. Simulations of energy

Next we illustrate the main features of energy evolution in tsunami generation. Kervella et al. [2007] showed that dispersive effects are usually negligible, especially for tsunamis generated by earthquakes. Therefore we restrict our study to the non-dispersive SWE (2.27)–(2.29). We solve these equations numerically with a finite volume method [Dutykh et al., 2008].

While the common practice in modeling tsunami generation consists in translating the initial sea bottom deformation to the water surface, thus neglecting all dynamical effects, we prefer to include some dynamics in the process in an effort to be closer to what happens in reality [Dutykh et al., 2006]. We construct the bottom motion by multiplying Okada's static solution $\zeta_{OK}^*(x^*, y^*)$ † by a function of time

† Okada solution is a steady analytical solution for the seafloor displacement following an underwater earthquake, based on dislocation theory in an elastic half-space [Okada, 1985].

Parameter	Value
Dip angle, δ	13°
Slip angle, θ	90°
Fault length, L^*	18 km
Fault width, W^*	14 km
Fault depth	5 km
Slip along the fault	10 m
Poisson ratio	0.27
Young modulus	9.5×10^9 Pa
Acceleration due to gravity, g	9.81 m/s^2
Water depth, h_0	1 km
Characteristic rise time, t_0^*	8 s
$\alpha^* = \log(3)/t_0^*$	0.1373 s^{-1}

Table 1. Values of physical parameters used for the energy density computations.

[Hammack, 1973]:

$$h^*(x^*, y^*, t^*) = h_0^*(x^*, y^*) - (1 - e^{-\alpha^* t^*}) \zeta_{OK}^*(x^*, y^*).$$

The parameter α^* is related to the characteristic time t_0^* under consideration. We chose

$$1 - e^{-\alpha^* t_0^*} = \frac{2}{3} \Leftrightarrow \alpha^* = \frac{\log 3}{t_0^*}.$$

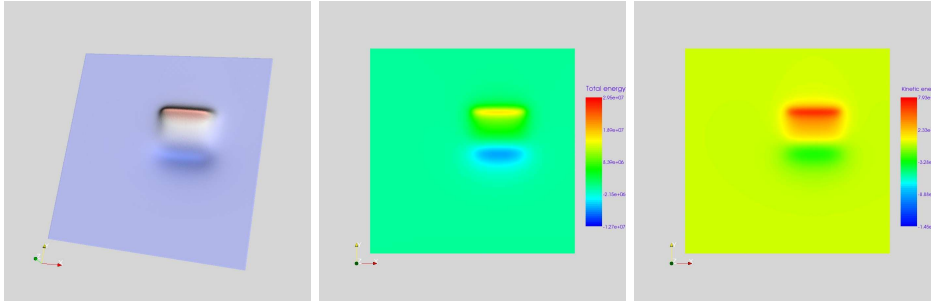
The various parameters used in the computations are given in Table 1.

Other time laws are possible and we refer to Dutykh and Dias [2007] for more details. In the present numerical computations we chose $h_0^*(x^*, y^*) = h_0 = \text{const}$. This choice is not only made for the sake of simplicity. Another reason is that Okada solution is derived within the assumption of an elastic half-space which does not take into account the bathymetry. In order to be coherent with this solution we assume the bottom to be flat before deformation.

Figures 2–9 show the distributions of free-surface elevation $\eta^*(x^*, y^*)$, total energy $E^*(x^*, y^*)$ and kinetic energy at various times. With our definition of potential energy, the energy is not zero at time $t^* = 0$:

$$E^*(t^* = 0) = E_0^* = \int_{-h_0}^0 \rho^* e^* dz^* = -\frac{1}{2} \rho^* g h_0^2.$$

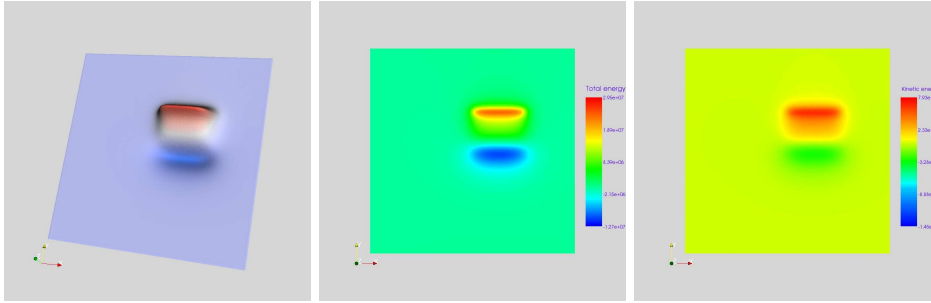
This value is used as initial condition. This is why the quantity $E^* - E_0^*$ is shown on the plots (b). The energy can be locally negative, indicating that energy is being transmitted from the water column to the solid bottom. One clearly sees the generation process. The formation of the leading elevation and depression waves takes a few seconds. Then the propagation begins. As shown by Ben-Menahem and Rosenman [1972], tsunami energy radiates primarily at right angles to a rupturing fault (see also Kajiura [1970]). During the formation of the wave, the distribution of kinetic energy does not change much, while the total energy increases in the water column below the elevation wave and decreases in the water column below



(a) Free surface

(b) Total energy

(c) Kinetic energy

Figure 2. Tsunami generation leading to a dipolar wave form. $t^* = 3$ s

(a) Free surface

(b) Total energy

(c) Kinetic energy

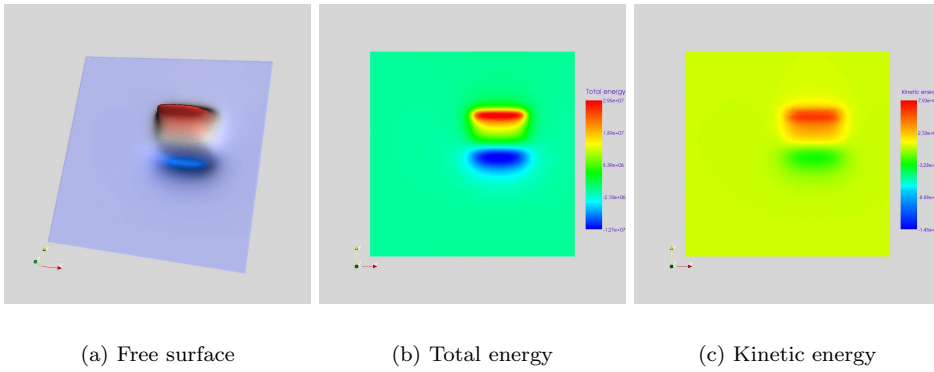
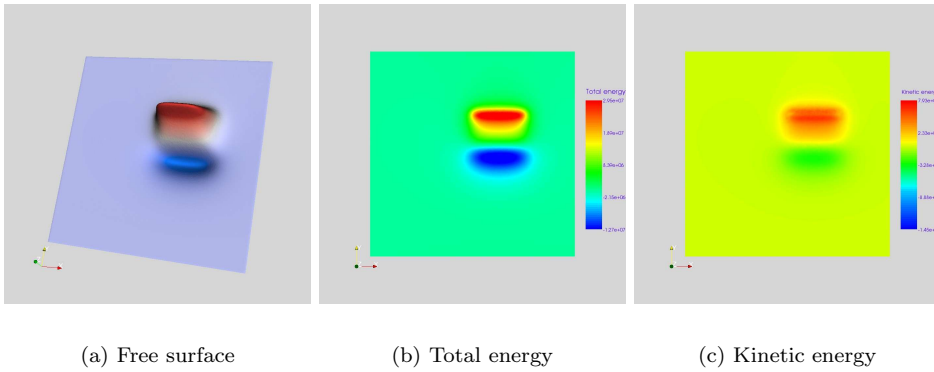
Figure 3. $t^* = 5$ s

the depression wave. When the waves start to propagate, the total energy remains roughly constant, while the kinetic energy increases in both waves.

It is also of interest to see how the total energy E^* , integrated over the whole fluid domain, varies during the generation process. This evolution is shown in figure 10. Two curves are plotted. The top curve simply is the energy (2.8) integrated over the water surface. The second curve is obtained as follows. Imagine that one is solving the SWE without the energy equation. In order to look at the energy, a natural way to do it is to approximate the energy $E^* - E_0^*$ as

$$E^* - E_0^* \approx \frac{1}{2}\rho^* H^* |\bar{\mathbf{u}}^*|^2 + \frac{1}{2}\rho^* g (\eta^{*2} - h^{*2}) + \frac{1}{2}\rho^* g h_0^2,$$

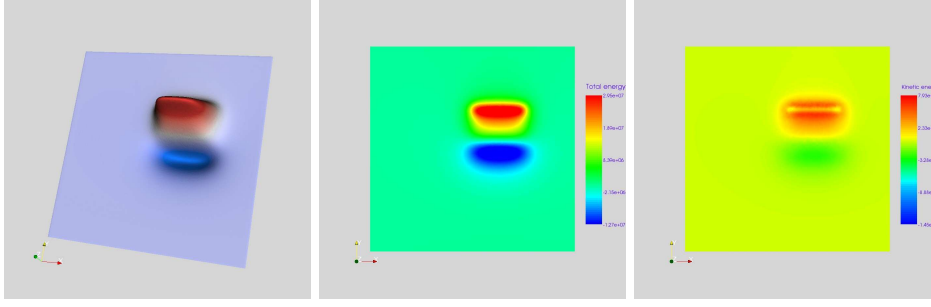
and then to integrate over the whole fluid domain. We see that the difference between the proper way to compute the energy and the approximate way can be large. It is probably due to the vertical velocity, which is completely neglected in the second approach. Once the motion of the sea bottom has stopped, the total energy remains constant.

Figure 4. $t^* = 8$ sFigure 5. $t^* = 10$ s

4. Energy in the framework of the dispersive linearized equations

In the case of tsunamis generated by earthquakes, nonlinear effects are not important during the process of generation and propagation. This is why it is valid to use the linearized water-wave equations. Dutykh et al. [2006] and others showed that taking an instantaneous seabed deformation is not equivalent to instantaneously transferring the seabed deformation to the ocean surface, except in the framework of the linearized shallow water equations (very long waves). The difference comes from the vertical velocities and dispersion. In this case we must go back to the initial set of equations (2.1)–(2.3). Since the motion starts from the state of rest, it can be considered as irrotational (potential flow) and one can introduce the velocity potential $\mathbf{u}^* = \nabla\phi^*$.

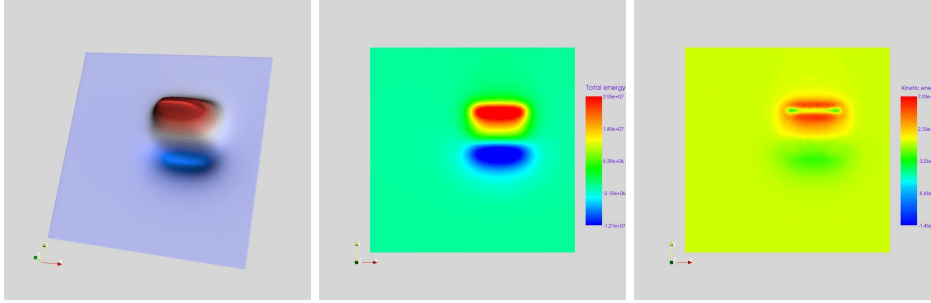
We perform the linearization of the equations (2.1) and (2.2), and of the boundary conditions (2.4)–(2.6). It is equivalent to taking the limit of the equations as $\varepsilon \rightarrow 0$. For the sake of convenience, we switch back the physical variables. The



(a) Free surface

(b) Total energy

(c) Kinetic energy

Figure 6. $t^* = 15$ s

(a) Free surface

(b) Total energy

(c) Kinetic energy

Figure 7. $t^* = 20$ s

linearized problem in dimensional variables reads [Dutykh and Dias, 2007]

$$\Delta\phi^* + \partial^2\phi^*/\partial z^{*2} = 0, \quad (x^*, y^*, z^*) \in \mathbb{R}^2 \times [-h^*, 0], \quad (4.1)$$

$$\frac{\partial\phi^*}{\partial z^*} = \frac{\partial\eta^*}{\partial t^*}, \quad z^* = 0, \quad \text{kinematic condition} \quad (4.2)$$

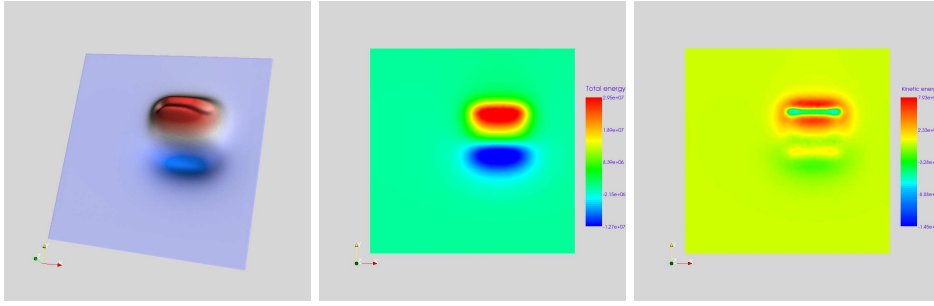
$$\frac{\partial\phi^*}{\partial t^*} + g\eta^* = 0, \quad z^* = 0, \quad \text{dynamic condition.} \quad (4.3)$$

Within linear theory the forces that cause perturbations are so weak that the boundary condition at the bottom (2.6) is also simplified:

$$\frac{\partial\phi^*}{\partial z^*} = \frac{\partial\zeta^*}{\partial t^*}, \quad z^* = -h^*. \quad (4.4)$$

The bottom motion appears in the right-hand side of equation (4.4).

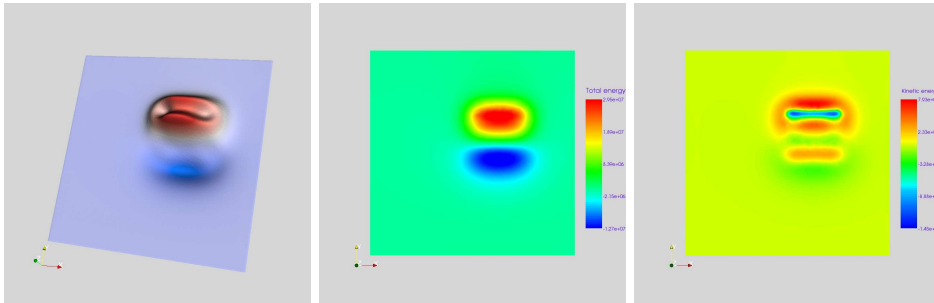
The Laplace equation (4.1) together with the boundary conditions (4.2), (4.3) and (4.4) determine the boundary-value problem for the velocity potential ϕ^* within the linear theory. In order to solve the equations for a prescribed bottom motion, one



(a) Free surface

(b) Total energy

(c) Kinetic energy

Figure 8. $t^* = 30$ s

(a) Free surface

(b) Total energy

(c) Kinetic energy

Figure 9. $t^* = 40$ s

can use Fourier and Laplace transforms (this approach is followed here) or Green's functions. Three scenarios are considered for the bottom motion [Dutykh et al., 2006]: the passive generation in which the deformation of the sea bottom is simply translated to the free surface (one is then solving an initial value problem) and two dynamical processes $\zeta^*(x^*, y^*, t^*) = T(t^*)\zeta_{OK}^*(x^*, y^*)$, where $\zeta_{OK}^*(x^*, y^*)$ is given by Okada's solution. The two choices for T are the instantaneous deformation with $T(t^*) = T_i(t^*) = \mathcal{H}(t^*)$, where $\mathcal{H}(t^*)$ denotes the Heaviside step function, and the exponential law used above in Section 3:

$$T(t^*) = T_e(t^*) = \begin{cases} 0, & t^* < 0, \\ 1 - e^{-\alpha^* t^*}, & t^* \geq 0, \end{cases} \quad \text{with } \alpha^* > 0.$$

Let $\widehat{\zeta}_{OK}^*$ be the Fourier transform of ζ_{OK}^* , $\omega^2 = g|\mathbf{k}^*| \tanh(|\mathbf{k}^*|h^*)$ the dispersion relation and $\mathbf{x}^* = (x^*, y^*)$. We provide the general integral solution for the free surface elevation in the three cases,

$$\eta_o^*(\mathbf{x}^*, t^*) = \frac{1}{(2\pi)^2} \iint_{\mathbb{R}^2} \widehat{\zeta}_{OK}^* e^{i\mathbf{k}^* \cdot \mathbf{x}^*} \cos(\omega t^*) d\mathbf{k}^*, \quad (\text{passive}) \quad (4.5)$$

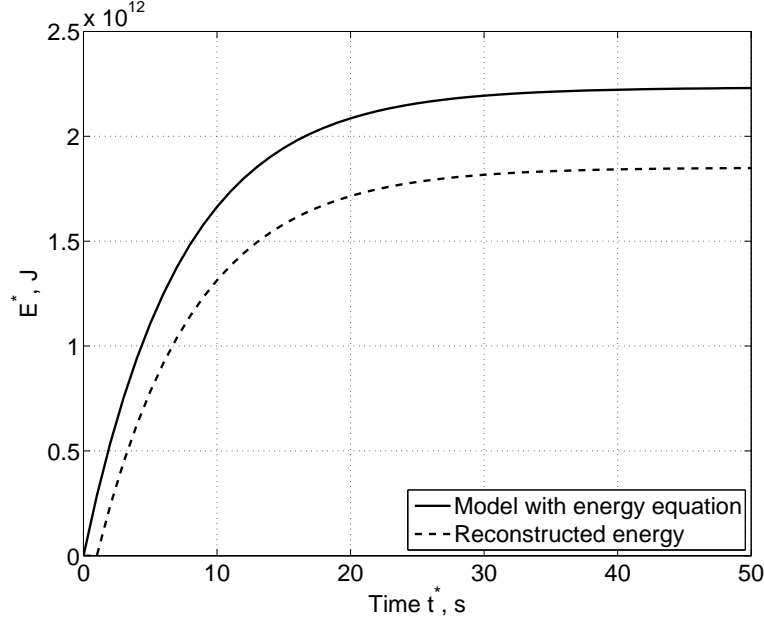


Figure 10. Total energy $\iint E^* d\mathbf{x}^*$ as a function of time computed with the SWE with energy (top curve) and reconstructed from the flow variables \bar{u}^* and η^* when no energy equation is used.

$$\eta_i^*(\mathbf{x}^*, t^*) = \frac{1}{(2\pi)^2} \iint_{\mathbb{R}^2} \frac{\widehat{\zeta}_{OK}^* e^{i\mathbf{k}^* \cdot \mathbf{x}^*}}{\cosh(|\mathbf{k}^*| h^*)} \cos(\omega t^*) d\mathbf{k}^*, \quad (\text{instantaneous}) \quad (4.6)$$

$$\eta_e^*(\mathbf{x}^*, t^*) = \frac{-\alpha^{*2}}{(2\pi)^2} \iint_{\mathbb{R}^2} \frac{\widehat{\zeta}_{OK}^* e^{i\mathbf{k}^* \cdot \mathbf{x}^*}}{\cosh(|\mathbf{k}^*| h^*)} \frac{e^{-\alpha^* t^*} - \cos(\omega t^*) - \omega/\alpha^* \sin(\omega t^*)}{\alpha^{*2} + \omega^2} d\mathbf{k}^*, \quad (4.7)$$

and the velocity potential in the passive case (the expressions for the other two active cases are a bit cumbersome) [Dutykh et al., 2006],

$$\phi_o^*(\mathbf{x}^*, t^*) = \frac{1}{4\pi^2} \iint_{\mathbb{R}^2} \frac{-g}{\omega} \widehat{\zeta}_{OK}^* e^{i\mathbf{k}^* \cdot \mathbf{x}^*} (\cosh |\mathbf{k}^*| z^* + \tanh |\mathbf{k}^*| h^* \sinh |\mathbf{k}^*| z^*) d\mathbf{k}^*. \quad (4.8)$$

Then one can easily compute the kinetic and potential energies:

$$E_K^* = \frac{1}{2} \rho^* \iint_{\mathbb{R}^2} \int_{-h^*}^{\eta^*} |\nabla \phi^*|^2 d\mathbf{x}^* dz^*, \quad E_P^* = \frac{1}{2} \rho^* g \iint_{\mathbb{R}^2} \eta^{*2} d\mathbf{x}^*. \quad (4.9)$$

Results are shown in figures 11 and 12. Even though there are differences during the first few seconds, the three mechanisms lead to the same almost exact equipartition between kinetic and potential energy once the dipolar waves start to propagate. The simplest estimate proposed for the energy of tsunamis generated by a dislocation source is that given by Okal and Synolakis [2003]. They compute the increase in potential energy of the ocean by displacing a volume of water $S \times \delta h^*$ from the

<i>Parameter</i>	<i>Value</i>
Dip angle, δ	13°
Slip angle, θ	90°
Fault length, L^*	150 km
Fault width, W^*	50 km
Fault depth	35 km
Slip along the fault	15 m
Poisson ratio	0.27
Young modulus	9.5×10^9 Pa
Acceleration due to gravity, g	9.81 m/s ²
Water depth, h^*	4 km
Characteristic rise time, t_0^*	50 s
$\alpha^* = \log(3)/t_0^*$	0.0220 s ⁻¹

Table 2. Values of physical parameters used for the Cauchy-Poisson analysis of tsunami generation.

bottom to the surface of the ocean. This also represents the work of the pressure forces displacing the ocean bottom. Then they explain that the center of mass of the displaced water, initially at height $\delta h^*/2$ above the ocean floor, is transferred to the ocean surface, so that the change in potential energy is not as much. The difference between the two is the energy available to the tsunami wave:

$$\iint E^* d\mathbf{x}^* = \frac{1}{2} \rho^* g S (\delta h^*)^2. \quad (4.10)$$

Incidentally, this expression does not depend on the sign of δh^* and is also valid for a sudden subsidence of a section of the ocean floor. It can be extended to a more realistic sea floor deformation, such as the one used in this paper, $\zeta_{OK}^*(x^*, y^*)$:

$$\iint E^* d\mathbf{x}^* = \frac{1}{2} \rho^* g \iint (\zeta_{OK}^*)^2 d\mathbf{x}^*. \quad (4.11)$$

This quantity corresponds to the square in figure 11(b).

5. Concluding remarks

In this article we provided a rigorous derivation of the total energy equation in the framework of the nonlinear SWE, both for dispersive and non-dispersive waves. We also made an attempt to better understand the energy transfer from a moving bottom to the water above. The importance of this topic is clear, given the serious hazard that tsunamis represent for coastal regions.

Tsunami energy can be studied at several levels. A simple formula was given by Okal and Synolakis [2003]. In the present paper, we extended it to more spatially realistic sea floor deformations. But this formula does not involve any dynamics, which can play an important role in tsunami generation. A somewhat counterintuitive consequence of this simple estimate is that the energy carried by the full tsunami wave is practically independent of depth [Okal and Synolakis, 2004]. One would think that the energy involved in lifting a 4 km column of water above a

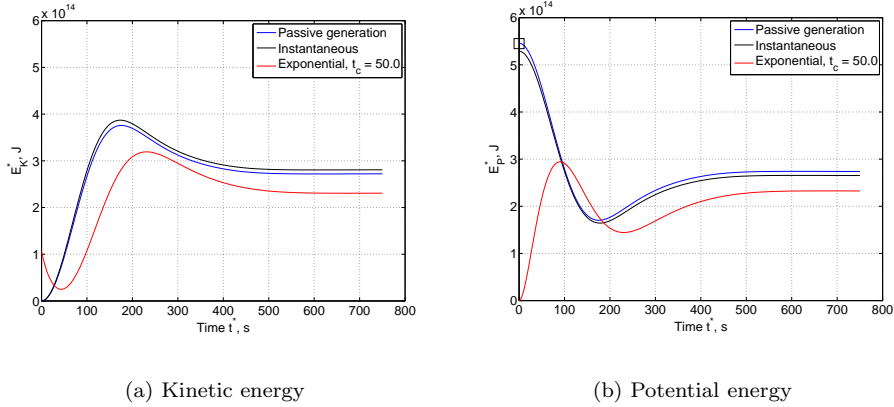


Figure 11. Time evolution of kinetic and potential energies for three mechanisms of tsunami generation: passive generation, instantaneous bottom motion and exponential bottom motion. The square in plot (b) indicates the estimate (4.11).

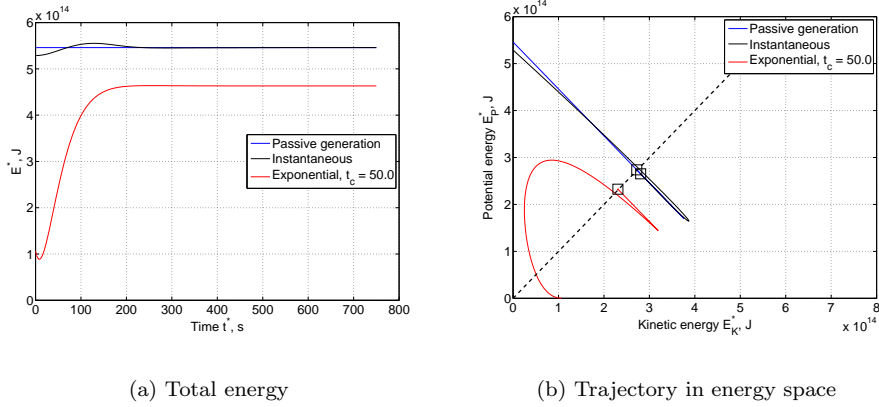


Figure 12. Same as figure 11. Time evolution of total energy (a) and trajectory in energy space (b). The dashed line represents equipartition of kinetic and potential energies. The squares represent the last computed points.

rupture is very different from lifting only 100 m of water (whether instantaneously or in a few seconds). But no difference can be found in wave height. The assumption of incompressibility may in fact no longer be valid, especially for a very deep ocean.

The emphasis of this paper has been on tsunami generation. At the runup or inundation stage, energy is also quite important. Potential energy is being transferred into kinetic energy and the study of these exchanges is left for future work. There are other aspects of tsunami energy: for example Berry [2007] looked at ray bending, which generally leads to focusing of the tsunami energy, with cusps developing on the front. Near the cusps the tsunami is more intense and therefore more destructive. The connections between our approach and Berry's approach should be investigated. The present paper can be considered as a first step towards a better

understanding of tsunami wave energy, in order to provide scales for tsunami magnitudes for example. More profound mathematical and physical analysis is needed.

Another extension is the study of other mechanisms. For example Okal [2003] showed that the combination of a lesser absolute level of excitation and a more pronounced shift of the spectral energy towards higher frequencies characterized by strong dispersion, makes landslide sources significantly deficient far-field tsunami generators, as compared to classical dislocations.

The authors would like to thank Jean-Michel Ghidaglia who suggested the idea to consider Boussinesq equations with energy. As well, we are grateful to him for numerous fruitful discussions on numerical and fluid mechanics topics. The second author acknowledges the support from the EU project TRANSFER (Tsunami Risk ANd Strategies For the European Region) of the sixth Framework Programme under contract no. 037058.

Appendix A. Derivation of dispersive shallow-water equations with variable bathymetry

We derive the Boussinesq equations following the method used, for example, by Nwogu [1993], Villeneuve and Savage [1993], Yoon and Liu [1989]. A moving bathymetry was considered in the framework of the Boussinesq equations by Villeneuve and Savage [1993], but they dealt with a 2D problem leading to a 1D system of equations.

We need to know the depth dependence of the horizontal velocity \mathbf{u}_\perp in order to reduce the problem to a 2D one. We expand \mathbf{u}_\perp in a Taylor series in the vertical coordinate z about the seabed $z = -h$:

$$\mathbf{u}(x, y, z, t) = \mathbf{u}|_{z=-h} + (z+h) \mathbf{u}_z|_{z=-h} + \frac{(z+h)^2}{2!} \mathbf{u}_{zz}|_{z=-h} + \dots \quad (\text{A } 1)$$

From now on, the horizontal velocity at the bottom is denoted by

$$\mathbf{u}_b := \mathbf{u}_\perp(x, y, -h, t).$$

If the flow is assumed to be irrotational, there is an additional relation which closes the system:

$$(\mathbf{u}_\perp)_z = \nabla w. \quad (\text{A } 2)$$

Substituting (2.22) into (A 2) clearly shows that $(\mathbf{u}_\perp)_z(x, y, -h, t) = O(\mu^2)$. Substituting (A 1) into (2.22) and integrating then yields

$$w = \mu^2 \zeta_t - \mu^2 \nabla \cdot ((z+h)\mathbf{u}_b) + O(\mu^4). \quad (\text{A } 3)$$

The vertical velocity varies linearly with respect to z over the depth at leading order $O(\mu^2)$.

The horizontal velocities can be found by integrating the irrotationality condition (A 2) from $-h$ to z :

$$\mathbf{u}_\perp = \mathbf{u}_b + \int_{-h}^z \nabla w \, dz. \quad (\text{A } 4)$$

Substituting (A 3) for w and integrating gives

$$\mathbf{u}_\perp = \mathbf{u}_b + \mu^2(z+h) \left[\nabla \zeta_t - \frac{1}{2}(z-h)\nabla(\nabla \cdot \mathbf{u}_b) - \nabla(\nabla \cdot (h\mathbf{u}_b)) \right] + O(\mu^4). \quad (\text{A } 5)$$

We see that the horizontal velocities vary quadratically with respect to z over the depth at leading order $O(\mu^2)$.

Following Ursell [1953], we introduce a number which measures the relative importance of nonlinear and dispersive effects in long waves:

$$S := \frac{\varepsilon}{\mu^2}.$$

In order to simplify the computations we now assume that $S = O(1)$. Dispersive terms can be neglected if $S \gg 1$.

An expression for the pressure can be obtained by substituting (A 5) and (A 3) into (2.21), integrating and retaining leading order terms:

$$\pi = \eta + \frac{\mu^2}{2} z^2 \nabla \cdot \mathbf{u}_{bt} + \mu^2 z (\nabla \cdot (h\mathbf{u}_{bt}) - \zeta_{tt}) + O(\mu^4). \quad (\text{A } 6)$$

The equation for the free-surface evolution is derived by substituting (A 5) into the depth-integrated continuity equation (2.19) and integrating:

$$\eta_t + \nabla \cdot ((h + \varepsilon\eta)\mathbf{u}_b) - \mu^2 \nabla \cdot \left[\frac{h^2}{2} \nabla(\nabla \cdot (h\mathbf{u}_b) - \zeta_t) - \frac{h^3}{3} \nabla(\nabla \cdot \mathbf{u}_b) \right] - \zeta_t = 0. \quad (\text{A } 7)$$

The equation for the evolution of the horizontal velocity is obtained by substituting (A 5) and (A 6) into (2.12) and (2.13):

$$\mathbf{u}_{bt} + \varepsilon(\mathbf{u}_b \cdot \nabla)\mathbf{u}_b + \nabla\eta + \mu^2 \left[\frac{h^2}{2} \nabla(\nabla \cdot \mathbf{u}_b) - h\nabla(\nabla \cdot (h\mathbf{u}_b) - \zeta_t) \right]_t = 0.$$

Using the irrotationality condition this equation can be rewritten as

$$\mathbf{u}_{bt} + \frac{\varepsilon}{2} \nabla |\mathbf{u}_b|^2 + \nabla\eta + \mu^2 \left[\frac{h^2}{2} \nabla(\nabla \cdot \mathbf{u}_b) - h\nabla(\nabla \cdot (h\mathbf{u}_b) - \zeta_t) \right]_t = 0. \quad (\text{A } 8)$$

Finally we write the energy equation by substituting (A 5) and (A 6) into (2.23):

$$\frac{\partial}{\partial t} \int_{-h}^{\varepsilon\eta} e \, dz + \varepsilon \nabla \cdot \left[\left(\int_{-h}^{\varepsilon\eta} e \, dz + \frac{1}{2}(h + \varepsilon\eta)^2 \right) \mathbf{u}_b \right] - \varepsilon(h + \varepsilon\eta)\zeta_t = 0. \quad (\text{A } 9)$$

The higher-order terms are of order $O(\varepsilon\mu^2)$.

Another possibility for the choice of variables is to introduce the depth averaged velocity. The corresponding standard Boussinesq-type equations were obtained by Peregrine [1967] in the case of a fixed seabed. We extend the results to a moving bathymetry and add the energy equation. The main advantage of the depth averaged velocity consists in the fact that the continuity equation (or equivalently the equation for the free-surface elevation) is very simple and exact in this variable.

Let us rewrite all equations in terms of the depth-averaged velocity defined by

$$\bar{\mathbf{u}} = \frac{1}{h + \varepsilon\eta} \int_{-h}^{\varepsilon\eta} \mathbf{u}_{\perp} dz. \quad (\text{A } 10)$$

The depth-integrated continuity equation (2.19) yields immediately

$$\eta_t + \nabla \cdot ((h + \varepsilon\eta)\bar{\mathbf{u}}) - \zeta_t = 0. \quad (\text{A } 11)$$

In order to derive equations for the horizontal velocity and the energy we need a relation between \mathbf{u}_b and $\bar{\mathbf{u}}$. The desired relation is deduced directly from the definition (A 10) by substituting (A 5) in it:

$$\bar{\mathbf{u}} = \mathbf{u}_b - \frac{\mu^2}{2} h \nabla (\nabla \cdot (h\mathbf{u}_b) - \zeta_t) + \frac{\mu^2}{3} h^2 \nabla (\nabla \cdot \mathbf{u}_b) + O(\varepsilon^2 + \varepsilon\mu^2 + \mu^4).$$

Inverting the last equation yields

$$\mathbf{u}_b = \bar{\mathbf{u}} + \mu^2 \left[\frac{h}{2} \nabla (\nabla \cdot (h\mathbf{u}_b) - \zeta_t) - \frac{h^2}{3} \nabla (\nabla \cdot \mathbf{u}_b) \right] + O(\varepsilon^2 + \varepsilon\mu^2 + \mu^4). \quad (\text{A } 12)$$

Substituting the relation (A 12) into equation (A 8) gives the standard Boussinesq equations for a moving bottom:

$$\bar{\mathbf{u}}_t + \frac{\varepsilon}{2} \nabla |\bar{\mathbf{u}}|^2 + \nabla \eta + \mu^2 \left[\frac{h^2}{6} \nabla (\nabla \cdot \bar{\mathbf{u}}) - \frac{h}{2} \nabla (\nabla \cdot (h\bar{\mathbf{u}}) - \zeta_t) \right]_t = 0. \quad (\text{A } 13)$$

The energy equation is obtained by substituting the relation (A 12) into equation (A 9):

$$\frac{\partial}{\partial t} \int_{-h}^{\varepsilon\eta} e dz + \varepsilon \nabla \cdot \left[\left(\int_{-h}^{\varepsilon\eta} e dz + \frac{1}{2} (h + \varepsilon\eta)^2 \right) \bar{\mathbf{u}} \right] - \varepsilon (h + \varepsilon\eta) \zeta_t = 0. \quad (\text{A } 14)$$

Since the energy equation is redundant for incompressible flows, the linear dispersion relation is unaffected by the inclusion of the energy equation. As is well-known, it can be improved by defining the horizontal velocity at an arbitrary level.

References

- A. Ben-Menahem and M. Rosenman. Amplitude patterns of tsunami waves from submarine earthquakes. *J. Geophys. Res.*, 77:3097–3128, 1972.
- M.V. Berry. Focused tsunami waves. *Proc. R. Soc. A*, 463:3055–3071, 2007.
- M.H. Dao and P. Tkalich. Tsunami propagation modelling - a sensitivity study. *Nat. Hazards Earth Syst. Sci.*, 7:741–754, 2007.
- D. Dutykh and F. Dias. Water waves generated by a moving bottom. In Anjan Kundu, editor, *Tsunami and Nonlinear Waves*, pages 63–94. Springer Verlag (Geo Sc.), 2007.

- D. Dutykh, F. Dias, and Y. Kervella. Linear theory of wave generation by a moving bottom. *C. R. Acad. Sci. Paris, Ser. I*, 343:499–504, 2006.
- D. Dutykh, R. Poncet, and F. Dias. Complete numerical modelling of tsunami waves: generation, propagation and inundation. *in preparation*, 2008.
- C. Eskilsson and S.J. Sherwin. Discontinuous Galerkin spectral/hp element modelling of dispersive shallow water systems. *J. Sci. Comp.*, 22-23:269–288, 2005.
- G.R. Gislér. Tsunami simulations. *Annu. Rev. Fluid Mech.*, 40:71–90, 2008.
- J. Hammack. A note on tsunamis: their generation and propagation in an ocean of uniform depth. *Journal of Fluid Mechanics*, 60:769–799, 1973.
- R. S. Johnson. *A modern introduction to the mathematical theory of water waves*. Cambridge University Press, Cambridge, 1997.
- K. Kajiwara. Tsunami source, energy and the directivity of wave radiation. *Bulletin of the Earthquake Research Institute*, 48:835–869, 1970.
- U. Kânoglu and C.E. Synolakis. Initial value problem solution of nonlinear shallow water-wave equations. *Phys. Rev. Lett.*, 97:148501, 2006.
- Y. Kervella, D. Dutykh, and F. Dias. Comparison between three-dimensional linear and nonlinear tsunami generation models. *Theoretical and Computational Fluid Dynamics*, 21:245–269, 2007.
- Z. Kowalik, W. Knight, T. Logan, and P. Whitmore. The tsunami of 26 December, 2004: Numerical modeling and energy considerations. *Pure and Applied Geophysics*, 164:379–393, 2007.
- E. Kulikov, P. Medvedev, and S. Lappo. Dispersion of the Sumatra tsunami waves in the Indian Ocean detected by satellite altimetry. *Trans. (Doklady) Russian Acad. Sci., Oceanology*, 401:537–542, 2005.
- O. Nwogu. Alternative form of Boussinesq equations for nearshore wave propagation. *J. Waterways Port Coastal Ocean Engng, ASCE*, 119:618–638, 1993.
- Y. Okada. Surface deformation due to shear and tensile faults in a half-space. *Bull. Seism. Soc. Am.*, 75:1135–1154, 1985.
- E. A. Okal. Normal mode energetics for far-field tsunamis generated by dislocations and landslides. *Pure Appl. Geophys.*, 160:2189–2221, 2003.
- E. A. Okal and C. E. Synolakis. A theoretical comparison of tsunamis from dislocations and landslides. *Pure Appl. Geophys.*, 160:2177–2188, 2003.
- E. A. Okal and C. E. Synolakis. Source discriminants for near-field tsunamis. *Geophys. J. Int.*, 158:899–912, 2004.
- E. A. Okal, J. Talandier, and D. Reymond. Quantification of hydrophone records of the 2004 Sumatra tsunami. *Pure Appl. Geophys.*, 164:309–323, 2007.
- D. H. Peregrine. Long waves on a beach. *J. Fluid Mech.*, 27:815–827, 1967.

- J. Ritsema, S. N. Ward, and F. I. González. Inversion of deep-ocean tsunami records for 1987 to 1988 Gulf of Alaska earthquake parameters. *Bulletin of the Seismological Society of America*, 85:747–754, 1995.
- J.J. Stoker. *Water waves, the mathematical theory with applications*. Wiley, 1958.
- C.E. Synolakis and E.N. Bernard. Tsunami science before and beyond Boxing Day 2004. *Phil. Trans. R. Soc. A*, 364:2231–2265, 2006.
- S. Tinti and E. Bortolucci. Energy of water waves induced by submarine landslides. *Pure Appl. Geophys.*, 157:281–318, 2000.
- V.V. Titov, A.B. Rabinovich, H.O. Mofjeld, R.E. Thomson, and F.I. González. The global reach of the 26 December 2004 Sumatra tsunami. *Science*, 309:2045–2048, 2005.
- F. Ursell. The long-wave paradox in the theory of gravity waves. *Proc. Camb. Phil. Soc.*, 49:685–694, 1953.
- M. Villeneuve and S.B. Savage. Nonlinear, dispersive, shallow-water waves developed by a moving bed. *Journal of Hydraulic Research*, 31(2):249–266, 1993.
- S.N. Ward. Relationship of tsunami generation and an earthquake source. *J. Phys. Earth*, 28:441–474, 1980.
- S.B. Yoon and P.L.-F. Liu. Interactions of currents and weakly nonlinear water waves in shallow water. *J. Fluid Mech.*, 205:397–419, 1989.